AT&T Technical Journal
Vol. 64, No. 10, December 1985
Printed in U.S.A.

Analysis/Simulation Study of Cross-Polarization Cancellation in Dual-Polarization Digital Radio

By L. J. GREENSTEIN*

(Manuscript received November 12, 1984)

This paper analyzes cross-polarization cancellation in dual-polarization digital radio links transmitting M-ary quadrature amplitude-modulation (M-QAM) signals. We consider the use of three options in the receiver: (1) no cancellation ; (2) ideal (i.e., total) cancellation; and (3) optimal nondispersive cancellation. For every option, we assume the canceler to be followed, in each polarization branch, by an ideal minimum mean-square error equalizer. By postulating a statistical model for the co-polarization and cross-polarization responses of a digital radio channel, and then simulating thousands of sets of these responses, we obtain curves that relate outage probability to the number of modulation levels. We show graphically that the no-canceler case is unthinkable; that total cancellation permits results close to those for single-polarization transmission; and that optimal nondispersive cancellation can have a limited range of application. We also examine the effects of key system parameters and the various modeling assumptions.

I. INTRODUCTION

This paper reports on a theoretical study of cross-polarization cancellation in dual-polarization microwave digital radio receivers. In another recent theoretical study, Amitay and Salz derived and evaluated the optimal linear receiver response to cross-pol coupling and multipath fading in combination.[1] By contrast, this paper analyzes suboptimal structures wherein the cross-pol canceler and multipath

* AT&T Bell Laboratories.

equalizer stages are in cascade. We do this because, in the design of practical adaptive receivers, it may be desirable to deal with cross-pol interference and co-pol dispersion separately. For example, cross-pol cancellation may be simpler to perform at IF, while multipath equalization is best done at baseband. More important, *modularity* in providing the cross-pol cancellation and multipath equalization functions may permit more economy and flexibility in designing and using the radio system.

Our primary aim is to show that, in using cross-pol cancellation followed by multipath equalization, overall outage performance can be made nearly as good as that for an equalized single-pol radio link. Our secondary aim is to quantify the differences in attainable outage performance for three distinct approaches to cancellation, namely, (1) no cancellation; (2) ideal (i.e., total) cancellation; and (3) optimal nondispersive cancellation. Finally, we aim to show how these results are influenced by key parameters of the system and various assumptions regarding the radio propagation.

To obtain these quantitative results, we use a combination of receiver analysis and Monte Carlo simulation of the co-pol and cross-pol responses of the propagation channel. The simulations require specifying a model for the channel responses. We have done so, despite the sparsity of published work in this area, by using data, tentative theories and speculations by the author and others. Model uncertainties are dealt with, in part, by means of sensitivity studies.

Our assumptions regarding the system, canceler/equalizer structure, and channel are given in Section II, while the methods of analysis and simulation are described in Section III. In Section IV, we present a number of simulation results in graphical form, and our major findings are summarized in Section V. The reader may wish to review this summary before plunging into the details of the study.

II. STUDY ASSUMPTIONS

2.1 The system

We consider digital radio links transmitting independent random data streams on two nominally identical cofrequency channels using nominally orthogonal polarizations. For reasons of both practicality and convenience, we assume the polarizations to be vertical (V-pol) and horizontal (H-pol).

The cofrequency channels are in the microwave common carrier bands at 4, 6, and 11 GHz, corresponding to channel bandwidths, respectively, of 20, 30, and 40 MHz. The modulation is M-ary Quadrature Amplitude Modulation (M-QAM), with M = 4, 16, 64, 256, etc. The end-to-end spectral shaping (excluding channel dispersion and

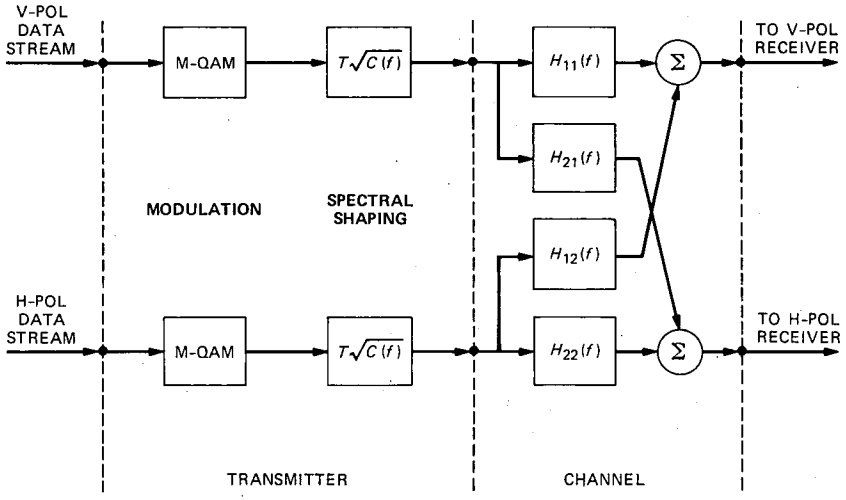

Fig. 1—Schematic representation of a dual-pol M-QAM transmitter with root-cosine-roll-off spectral shaping and a microwave channel with co-pol dispersion and cross-pol coupling. The H-functions are slowly time varying during periods of multipath activity.

adaptive filtering) is cosine roll-off, with roll-off factor α. This shaping is divided evenly between transmitter and receiver. In the receiver, the H-pol and V-pol signals are applied to a cross-pol canceler that linearly combines the two input branches, followed by fixed filtering and adaptive equalization in each output branch.

The above description is reflected in Figs. 1 and 2.* Figure 1 depicts the transmitter and channel, the latter being characterizable by a pair of co-pol responses [$H_{11}(f)$ for the V-pol signal and $H_{22}(f)$ for the H-pol signal] and a pair of cross-coupling responses [$H_{12}(f)$ and $H_{21}(f)$]. Ideally (and in fact under normal conditions), $H_{11}(f)$ and $H_{22}(f)$ are identical nondispersive responses. During multipath fading, however, they become dispersive and possibly smaller as well, as recounted in numerous papers on statistical models.[2-5]

The cross-pol responses, on the other hand, are ideally zero. In fact, however, they are generally nonzero, even under normal conditions. During such times, they are typically nondispersive and small compared to the co-pol responses; but, during multipath fading, they tend to be dispersive and can become relatively large as well,[6] giving rise to potentially serious impairments in detection.

Figure 2 shows the structure of the receiver to be analyzed. All the G-functions are adaptive, and we assume they can be controlled in practice to satisfy the various criteria specified below. For convenience

* Note that f is referred to the center frequency of the radio channel, and that $C(f)$ represents the raised cosine function (dimensionless).

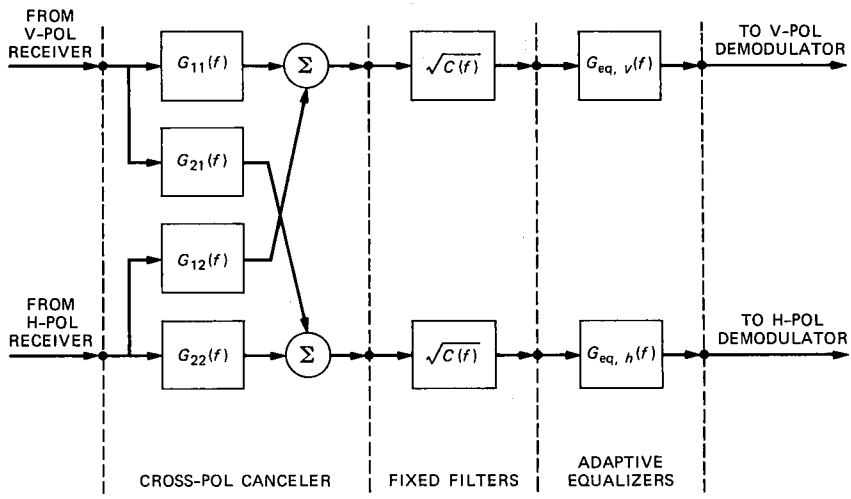

Fig. 2—Schematic representation of dual-pol receiver processing consisting of cross-pol cancellation, root-cosine-roll-off filtering, and adaptive equalization. The G-functions are assumed to be adapted to the prevailing channel response functions in Fig. 1. In principle, the location of the fixed filtering is immaterial, and each of the various linear stages can be at RF,IF or baseband, as appropriate.

only, all the processing stages are shown as passband (rather than baseband) circuits.

Finally, we assume in this study that the RF carriers and the symbol timings are nominally identical but asynchronous. This assumption enables the cross-pol interference to be treated as a noise-like process, which simplifies the analysis in some respects. The results should differ little from those for synchronized dual-pol transmissions.

2.2 Canceler/equalizer structure

To evaluate the canceler/equalizer structure, we need some analytical relationships. Let $S_V(f)$ be the Fourier transform of a long random sequence of (complex) data into the V-pol transmit filtering (Fig. 1), and let $S_H(f)$ be the same for the H-pol branch. Because of cross-coupling in both the propagation medium and the receiver, each branch will show a mixture of V-pol and H-pol data streams at its equalizer output (Fig. 2). Because of symmetry, however, we need only consider the output of the V-pol branch, and will follow that custom throughout.

The Fourier transform of the equivalent baseband signal at the V-pol output is

$$S'_V = S_V(f)C(f)\{[H_{11}(f)G_{11}(f) + H_{21}(f)G_{12}(f)]G_{eq,v}(f)\} + S_H(f)C(f)\{[H_{12}(f)G_{11}(f) + H_{22}(f)G_{12}(f)]G_{eq,v}(f)\}. \quad (1)$$

The second term clearly represents the *cross-pol interference* (hereafter

abbreviated CPI); the bracketed quantity of the first term represents the changes in the desired signal due to the propagation medium, canceler, and equalizer. If $H_{11}(f) = H_{22}(f) = 1$ and $H_{12}(f) = H_{21}(f) = 0$, $S_V'(f)$ reduces to the case of an undistorted single-pol transmission.

We now state the three conditions on $G_{11}(f)$ and $G_{12}(f)$ that will be analyzed here:

1. No cancellation, i.e.,

$$G_{11}(f) = 1 + j0; \qquad G_{12}(f) = 0. \tag{2}$$

2. Ideal cancellation, i.e., from (1),

$$\frac{G_{12}(f)}{G_{11}(f)} = -\frac{H_{12}(f)}{H_{22}(f)}. \tag{3}$$

3. Optimal nondispersive cancellation, defined here by

$$G_{11}(f) = 1 + j0; \qquad G_{12}(f) = g_{\text{opt}}, \tag{4}$$

where g_{opt} is that complex value for which the mean square CPI at the canceler output is minimized. There are other possible criteria for defining g_{opt} (e.g., that value that minimizes the mean-square CPI at the equalizer output), but the simple criterion used here is good enough for our purposes.

Finally, we assume that the equalizer associated with each of the above three conditions is an ideal Minimum Mean-Square Error (MMSE) equalizer. That is, it maximizes the ratio of the signal half-distance to the total root-mean-square (rms) distortion (thermal noise, CPI, and intersymbol interference) as sampled at the baseband detector. Previous studies for single-pol channels have shown that the performance of an ideal MMSE equalizer can be closely approached using fractionally spaced tapped-delay-line filters with just a few taps.[7]

2.3 Channel model

Obtaining an empirical statistical model for the four channel response functions—$H_{11}(f)$, $H_{12}(f)$, $H_{21}(f)$ and $H_{22}(f)$—is a very difficult business. The model to be used here is based only partly on measured data, the other parts being theories on the underlying physics of the propagation medium, and speculations on what mathematical artifacts to include so that important issues are not overlooked. The model draws on the published data, models or ideas of N. Amitay,[1] W. D. Rummler,[2,3] K. T. Wu,[6] S. Lin,[8] M. L. Steinberger[9] and M. Liniger,[10] as well as on private discussions with these investigators and others. The author's own ideas are included in the mixture, and he accepts sole responsibility for flaws in the speculative model presented next.

2.3.1 The co-pol functions, $H_{11}(f)$ and $H_{22}(f)$

The co-pol responses can be represented using the three-path function introduced by Rummler.[2] For most of the year, $H_{11}(f) = H_{22}(f) = 1$; but, during T_0 seconds per hop per year, the two functions become

$$H_{ii}(f) = \begin{cases} a_{ii}[1 - b_{ii}e^{j\phi_{ii}}e^{-j\omega\tau}]; & \text{minimum phase response} \\ a_{ii}[b_{ii} - e^{j\phi_{ii}}e^{-j\omega\tau}]; & \text{nonminimum phase response} \end{cases} \quad (5)$$

$$i = 1, 2,$$

where T_0 is a function of the radio path and band; τ is a fixed parameter of 6.3 ns; $(a_{11}, a_{22}, b_{11}, b_{22}\phi_{11}, \phi_{22})$ are slowly varying "fitting" parameters that collectively provide accurate approximations to the true responses; $b_{11} \leq 1$ and $b_{22} \leq 1$ at all times; and these representations apply over bandwidths of 40 MHz or less.

Rummler[3] has published a widely used joint probability density function (pdf) for the a-, b-, and ϕ-parameters of a co-pol function such as (5). We will use that pdf to characterize the statistics of both $H_{11}(f)$ and $H_{22}(f)$. Moreover, we assume each function to be minimum phase over a fraction p of all fade events, with p a parameter lying between 0 and 1.

In evaluating the dual-pol receiver, it will be necessary to assume something about the similarity *in time* between $H_{11}(f)$ and $H_{22}(f)$. According to a limited body of data, these functions tend to track quite closely, i.e., $H_{12}(f) \approx H_{11}(f)$ during most fade events. On the other hand, significant impairments could accrue during those events where they are dissimilar. To bracket the range of possibilities, we have obtained simulation results under two distinct assumptions: $H_{22}(f) = H_{11}(f)$ in every fade event; and $H_{11}(f)$ and $H_{22}(f)$ are *statistically* identical but mutually independent over the ensemble of fade events.

2.3.2 Cross-pol functions, $H_{12}(f)$ and $H_{21}(f)$

The model to be used here assumes that

$$H_{ij}(f) = \{0.5k_{ij}[H_{11}(f) + H_{22}(f)] + \epsilon_{ij}e^{j\psi_{ij}}\}e^{-j\omega\delta T}, \quad i \neq j \quad (6)$$

where k_{ij} is a fixed complex constant related to the residual cross-pol coupling in the radio antennas and waveguide runs (typically, 20 $\log|k_{ij}| \leq -25$ dB); ψ_{ij} is a uniformly random phase over the ensemble of fade events; ϵ_{ij} is a Rayleigh variate over that ensemble (typically, 10 $\log|\overline{\epsilon_{ij}}|^2 \leq -35$ dB); and δT is a fixed time "misalignment" between the co-pol and cross-pol paths to the receiver. We further assume that

ψ_{12}, ψ_{21}, ϵ_{12}, and ϵ_{21} are jointly independent, and that $k_{12} = k_{21}$, both real.*

This model for the cross-pol responses is more or less consistent with data and theories reported previously.[6,8–10] The delay parameter δT is new and is included to add richness to the model; we will see if δT has any important effects on performance as it ranges from 0 to 4 ns. This way of including delay effects may, in fact, be too mild. Amitay[1] has suggested that δT might be larger than 4 ns, and that the factor $e^{-j\omega\delta T}$ might more properly be attached to just $\epsilon_{ij}e^{j\phi_{ij}}$. Such an approach would make the cross-pol responses more dispersive, consistent with some reported measurements. For now, however, we will use the model for cross-pol responses described above.

III. METHODS OF ANALYSIS AND SIMULATION

3.1 Preliminaries

To begin, we note that an M-QAM signal contains two $\sqrt{M}$-level AM signals in phase quadrature, and that the possible data values in each quadrature rail are $\pm 1, \pm 3, \cdots \pm (\sqrt{M} - 1)$. We also note that, after cross-pol cancellation, fixed filtering, adaptive equalization, and coherent demodulation (in whatever order), two baseband pulse streams are sampled every T seconds at each of two data detectors in the V-pol receiver branch, and similarly for the H-pol receiver branch. Our analytical goal is to derive a signal-to-distortion ratio that characterizes performance at either baseband detector of either receiver branch. To the maximum extent possible, we invoke known relationships and any simplifying assumptions that do not compromise the generality of the results.

One simplifying assumption, noted and explained in Section 2.1, is that the cross-pol interference can be treated as a noise-like process. Another simplification accrues by assuming a zero-percent roll-off factor ($\alpha = 0$) for the end-to-end spectral shaping, in which case $C(f)$ is a unit rectangle on the f-interval $[-1/2T, 1/2T]$. This simplifying assumption is justified by earlier findings that, over the practical range $\alpha \leq 0.5$, the roll-off factor has a very mild effect on performance results.[11]

Finally, for convenience we define a carrier-to-noise ratio as follows: let P_0 be the average received power in an M-QAM signal in the absence of fading; and let N_0 be the power spectrum density of the

* The effects of the phases of k_{12} and k_{21}, and of any dissimilarities between these two constants, should be small. We thus remove them from the study to simplify matters.

noise input to the V-pol (or H-pol) receiver, including the contribution of the receiver noise figure. Then

$$\text{CNR} \triangleq P_0 T / N_0. \tag{7}$$

This is the unfaded Carrier-to-Noise Ratio (CNR) in the Nyquist bandwidth, and is typically on the order of 10^6 (60 dB).

3.2 Signal and distortions at the canceler output

From previous discussions and Figs. 1 and 2, we can show that the data pulse at the canceler output for a data value of unity would have a Fourier transform

$$S(f) = \sqrt{\frac{3}{M-1}}\, P_0\, (T\sqrt{C(f)})A(f), \tag{8}$$

where [see (1)]

$$A(f) = [H_{11}(f)G_{11}(f) + H_{21}(f)G_{12}(f)]. \tag{9}$$

Similarly, the thermal noise at that output has a power spectrum density

$$N(f) = N_0 B_n(f), \tag{10}$$

where (see Fig. 2)

$$B_n(f) = [|\, G_{11}(f)\,|^2 + |\, G_{12}(f)\,|^2]. \tag{11}$$

The cross-pol interference has a power spectrum density

$$X(f) = P_0 T C(f) B_c(f), \tag{12}$$

where [see (1)]

$$B_c(f) = |\, H_{12}(f)G_{11}(f) + H_{22}(f)G_{12}(f)\,|^2. \tag{13}$$

The composite noise power spectrum density* can then be written as

$$\begin{aligned} N'(f) &= N(f) + X(f) \\ &= N_0[B_n(f) + \text{CNR}\ C(f)B_c(f)]. \end{aligned} \tag{14}$$

Henceforth, we will make use of our assumption that $\alpha = 0$, i.e., that $C(f)$ is a unit rectangle on $[-1/2T, 1/2T]$.

3.3 The MMSE equalizer

The MMSE equalizer is the linear filter that maximizes, at the

* This spectrum density is for the sum of CPI and thermal noise, which can be treated as noise-like but is clearly not Gaussian except when the CPI vanishes.

baseband detector, the ratio of sampled-signal half-distance to rms distortion, the latter consisting of thermal noise, CPI, and Intersymbol Interference (ISI). We need not concern ourselves with how such an equalizer is realized, as this is a well-developed art; we merely need to derive and analyze its frequency response.

The derivation is accomplished in two steps. First, we assume a noise-whitening input filter, i.e., one having a real transfer function proportional to $1/\sqrt{N'(f)}$, and then we invoke the result in Section 5.1 of Ref. 12 for MMSE equalizers with white input noise. The equalizer response for $\alpha = 0$ turns out to be

$$G_{eq}(f) = \frac{A^*(f)}{B_n(f) + \mathrm{CNR}[B_c(f) + |A(f)|^2]}; \qquad |f| \leq \frac{1}{2}T$$
$$= 0; \qquad \text{elsewhere,} \tag{15}$$

where, for convenience, we have suppressed the subscript v in $G_{eq,v}(f)$, Fig. 2.

The data pulse following an equalizer with this response has a real, nonnegative Fourier transform. Assuming optimal carrier and timing recovery, we can show that the squared half distance between adjacent signal samples (constellation points) at the detector is therefore

$$P_s = [\int S(f)G_{eq}(f)df]^2, \tag{16}$$

where the integration limits, both here and in subsequent expressions, are $\pm 1/2T$.

The mean-square intersymbol interference at the sample times can likewise be shown to be

$$P_i = \frac{M-1}{3}\left[\frac{1}{T}\int |S(f)G_{eq}(f)|^2 df - P_s\right] \tag{17}$$

and the mean-square composite noise power is

$$P_{n'} = \int N'(f)|G_{eq}(f)|^2 df. \tag{18}$$

3.4 The signal-to-distortion parameter, Γ

The signal-to-distortion ratio (ρ) at either baseband detector is now defined to be

$$\rho \triangleq P_s/(P_i + P_{n'}). \tag{19}$$

The significance of ρ is that the Bit Error Rate (BER) can be tightly upperbounded by[1,13]

$$\mathrm{BER} \leq 2\exp(-\rho/2). \tag{20}$$

By using the various relationships in Sections 3.1 through 3.3, we can express ρ in the form

$$\rho = \frac{3}{M-1}\left(\frac{X_s}{X_i + X_{n'}/\mathrm{CNR}}\right) \equiv \frac{3}{M-1}\,\Gamma, \tag{21}$$

where

$$X_s \triangleq \left\{\overline{\left[\frac{Y(f)}{1 + \mathrm{CNR}\ Y(f)}\right]}\right\}^2 \tag{22}$$

$$X_i \triangleq \left\{\overline{\frac{Y(f)}{1 + \mathrm{CNR}\ Y(f)}}\right\}^2 - X_s \tag{23}$$

$$X_{n'} \triangleq \left\{\overline{\frac{Y(f)}{[1 + \mathrm{CNR}\ Y(f)]^2}}\right\} \tag{24}$$

$$Y(f) \triangleq |A(f)|^2/[B_n(f) + \mathrm{CNR}\ B_c(f)], \tag{25}$$

and the overbar denotes a frequency average over $[-1/2T, 1/2T]$, i.e.,

$$\overline{Z(f)} \triangleq \int_{-1/2T}^{1/2T} Z(f)\,df T. \tag{26}$$

The focus of our investigation is the signal-to-distortion parameter Γ introduced by (21). To "calibrate" this quantity, let Γ_0 denote the value of Γ that must be exceeded if BER is to lie below some threshold value BER_0. We can find a tight upperbound for Γ_0 given BER_0 and M by invoking the equality in (20) and combining it with (21). The result is

$$\Gamma_0 = \frac{2}{3}\,(M-1)\ell n(2/\mathrm{BER}_0). \tag{27}$$

Some values of Γ_0, expressed in decibles, are given in Table I for various BER_0 and M of interest.

3.5 Two special cases

Although the above results are applicable to any assumptions we make about the canceler, two special cases are worthy of note. The

Table I—Values of Γ_0 for various M and specified bit error rates

	M		
BER_0	16	64	256
10^{-3}	18.81 dB	25.04 dB	31.11 dB
10^{-4}	19.96 dB	26.19 dB	32.26 dB
10^{-5}	20.87 dB	27.10 dB	33.17 dB
10^{-6}	21.62 dB	27.85 dB	33.92 dB

first is the case of total cancellation [see (3)]. Under this condition, $X(f)$ in (12) vanishes entirely and so $N'(f)$ reduces to $N(f)$. Also, as the mathematics of this situation makes clear, the choices of $G_{11}(f)$ and $G_{12}(f)$ individually are immaterial, just so their ratio satisfies (3). This is a consequence of the (presumed) fact that the dominant thermal noise is introduced before the canceler.

The second special case is that of nondispersive cancellation [see (4)]. We assume that g_{opt} is chosen so as to minimize $\overline{X(f)}$ [see (12) and (13)]. For a zero-percent roll-off factor, it is easy to show that

$$g_{\text{opt}} = -\frac{\overline{H_{22}^*(f)H_{12}(f)}}{\overline{|H_{22}(f)|^2}}. \tag{28}$$

We have used this relationship in our computations.

3.6 Analysis/simulation program

For convenience in what follows, we now redefine two parameters of the channel model, namely,

$$K \triangleq 20 \log k, \tag{29}$$

where $k = k_{12} = k_{21}$ (real) in (6) and

$$E \triangleq 10 \log\overline{|\epsilon_{12}|^2} = 10 \log\overline{|\epsilon_{21}|^2}. \tag{30}$$

We can say that the channel is statistically specified once we (1) assign numerical values to p, δT, K and E; and (2) declare $H_{11}(f)$ and $H_{22}(f)$ to be either identical or statistically independent. Similarly, we can say that the radio system is design-specified once we (1) assign numerical values to α, CNR, and $1/T$; and (2) declare the type of cross-pol cancellation to be used.

A computer program has been written that obtains, for any joint specification of the channel and system, the yearly probability distribution of Γ. To accomplish this, the program combines Monte Carlo simulation methods with the channel model of Section 2.3 to generate a large statistical "ensemble" of channel response functions. That is, each member of the ensemble is a set of functions, $\{H_{11}(f), H_{12}(f), H_{21}(f), H_{22}(f)\}$, generated by deriving the various parameter values (a_{11}, b_{11}, a_{22}, b_{22}, ϵ_{12}, ϵ_{21}, etc.) in accordance with the statistics of the model. For each set of H-functions thus generated, the program computes Γ using the formulas of Section 3.4. After generating and evaluating the prescribed number of sets (20,000 in our study), the program computes a cumulative probability function, $P(\Gamma)$, for the population of Γ-values thus obtained.

We present results for the following channel/system parameter values or conditions, where those in boldface are the ones used the most extensively:

Minimum phase probability, p: 0, **0.5** and 1.0.
Delay parameter, δT: 0, **2 ns** and 4 ns.
Proportional coupling parameter, K: **−25 dB,** −30 dB, and −35 dB.
Additive coupling parameter, E: −35 dB, **−40 dB,** and −45 dB.
Statistical dependence between co-pol functions: **Totally dependent ($H_{11}(f) = H_{22}(f)$)** and totally independent.
Type of cancellation: No cancellation, **total cancellation**, and **nondispersive cancellation.**
Symbol rate, $1/T$: 15 Mbaud, **22.5 Mbaud,** and 30 Mbaud (typical values for digital radio systems in the 4-, 6-, and 11-GHz radio bands, respectively).

Throughout our simulations and computations, we have assumed a 0-percent roll-off factor ($\alpha = 0$) and a 63-dB unfaded carrier-to-noise ratio (CNR $= 2 \times 10^6$). However, we will also discuss how the computed results would vary with these parameters.

IV. RESULTS

The results of this study are given by Figs. 3 through 6. Each figure shows curves of $P(\Gamma)$ versus Γ for a number of different channel/system specifications. These curves can be interpreted as conditional outage probabilities and can be used to estimate yearly outage seconds on a radio hop, as follows: Given a threshold bit error rate (BER_0) and the number of modulation levels (M), the minimum acceptable value of Γ can be obtained using (27) or Table I. (Assuming $BER_0 = 10^{-4}$, Γ_0 is roughly 20 dB for $M = 16$ and 26 dB for $M = 64$.) The resulting $P(\Gamma_0)$ is the probability of outage on a given hop *conditioned* on the occurrence of fading. To estimate yearly outage seconds on the hop, one would need to estimate, measure, or obtain from available models the expected number of yearly fading seconds, T_0. (A representative value is 16,000 seconds.) Multiplying T_0 by $P(\Gamma_0)$ would yield the expected number of outage seconds per hop per year. This utilitarian aspect of the curves in Figs. 3 through 6 should be kept in mind as we make some relative comparisons.

4.1 Influence of symbol rate and type of cancellation

Figure 3 shows $P(\Gamma)$ for each of three symbol rates and each of three cancellation options. The "common conditions" listed on the figure are assumed to be the most representative for an actual dual-pol channel.

The top curve shows what can be expected if no cancellation whatsoever is employed. The heavy line used here contains the results for all symbol rates from 15 Mbaud to 30 Mbaud. It is clear that the absence of some sort of cancellation is unthinkable for the dual-pol

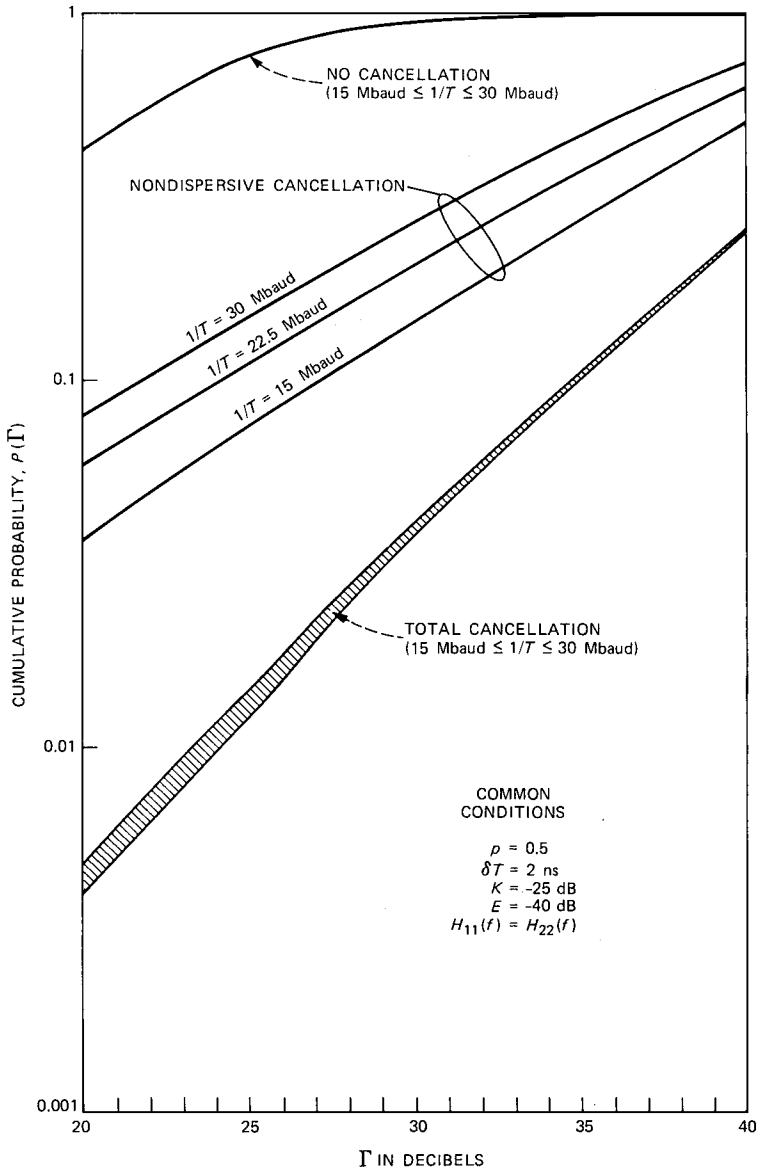

Fig. 3—Cumulative probability functions for Γ. Results are shown for each of the three canceller options considered and for symbol rates of 15, 22.5, and 30 Mbaud. In addition to the "common conditions" shown, $\alpha = 0$ and CNR $= 2 \times 10^6$ (63 dB).

systems of interest, and we dismiss this option from further consideration.

The results for nondispersive cancellation reveal an order-of-magnitude improvement (for the lower values of Γ) and a fairly strong

dependence on symbol rate. The latter is not surprising since larger symbol rates involve larger bandwidths and, hence, greater dispersion in the channel H-functions. In microwave common carrier channels with narrow bandwidths (e.g., 3.6 MHz in the 2-GHz band), nondispersive cancellation might thus be quite adequate. This would depend, of course, on the number of modulation levels and the outage probability requirements.

The narrow band at the bottom, for the case of total cancellation, contains results for all symbol rates between 15 Mbaud and 30 Mbaud. This approach provides, at the lower values of Γ, another order-of-magnitude improvement beyond nondispersive cancellation. Moreover, the dependence on symbol rate (or bandwidth) is seen to be small. Later, we will compare these results with those for single-pol transmission using ideal MMSE equalization.

4.2 *Influence of channel parameters p and δT*

Figure 4 shows results for both nondispersive and total cancellation as p and δT range over the sets of values we have specified for them. The "common conditions" assumed here are typical ones; alternative realistic assumptions would not alter the trends revealed by these curves.

The main conclusion we can draw here is that outage performance for nondispersive cancellation is sensitive to the details of the channel model, while that for total cancellation is not. This is reflected in the wideness and narrowness, respectively, of the bands for these two cases. Since total cancellation is the obvious design choice for a high-quality system, this is good news. It implies that certain hard-to-determine fine details of the channel model need not be accurately specified to obtain reliable performance estimates.

4.3 *Influence of the dependence between co-pol responses*

Figure 5 illustrates, for both nondispersive and total cancellation, how performance is affected by the statistical dependence between $H_{11}(f)$ and $H_{22}(f)$. The performance variation over the range between total dependence $[H_{11}(f) = H_{22}(f)]$ and total independence is seen to be fairly small. Nevertheless, it would be clearly beneficial if the co-pol responses were more independent than they apparently are.

A simple explanation can be given for the improvement shown when $H_{11}(f)$ and $H_{22}(f)$ are independent. Let us consider the case of total cancellation and assume, for simplicity, that all H-functions are essentially flat with frequency. Combining (10) and (11) with (3) and (1) under these circumstances, we can show that the receiver output

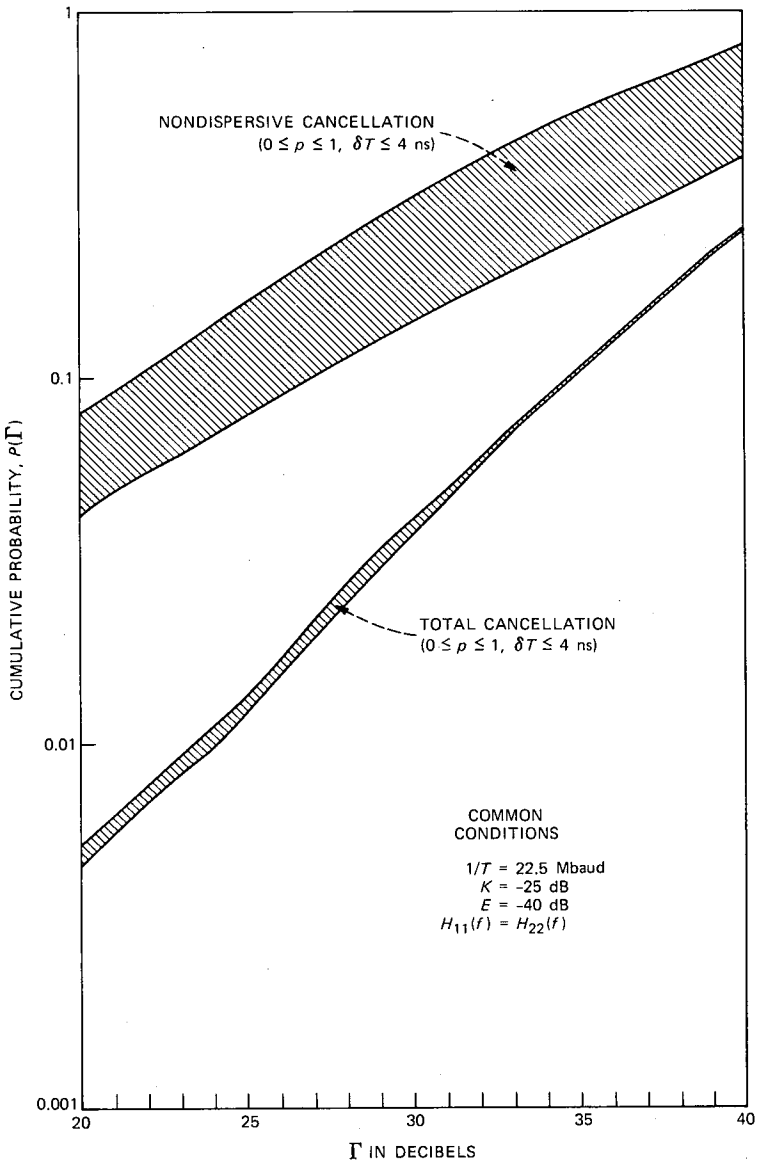

Fig. 4—Cumulative probability functions for Γ. Results are shown for nondispersive and total cancellation, with the symbol rate fixed at 22.5 Mbaud. The parameters here are the minimum phase probability (p) and the delay parameter (δT). All else is the same as in Fig. 3.

signal-to-noise ratio would be proportional to $|H_{11}H_{22} - H_{12}H_{21}|^2/[|H_{22}|^2 + |H_{12}|^2]$. The potential benefit of statistical independence arises when $|H_{11}|$ is weak; at such times, the numerator can be quite small if $|H_{22}|$ is similarly weak, via near cancellation of $H_{11}H_{22}$ by

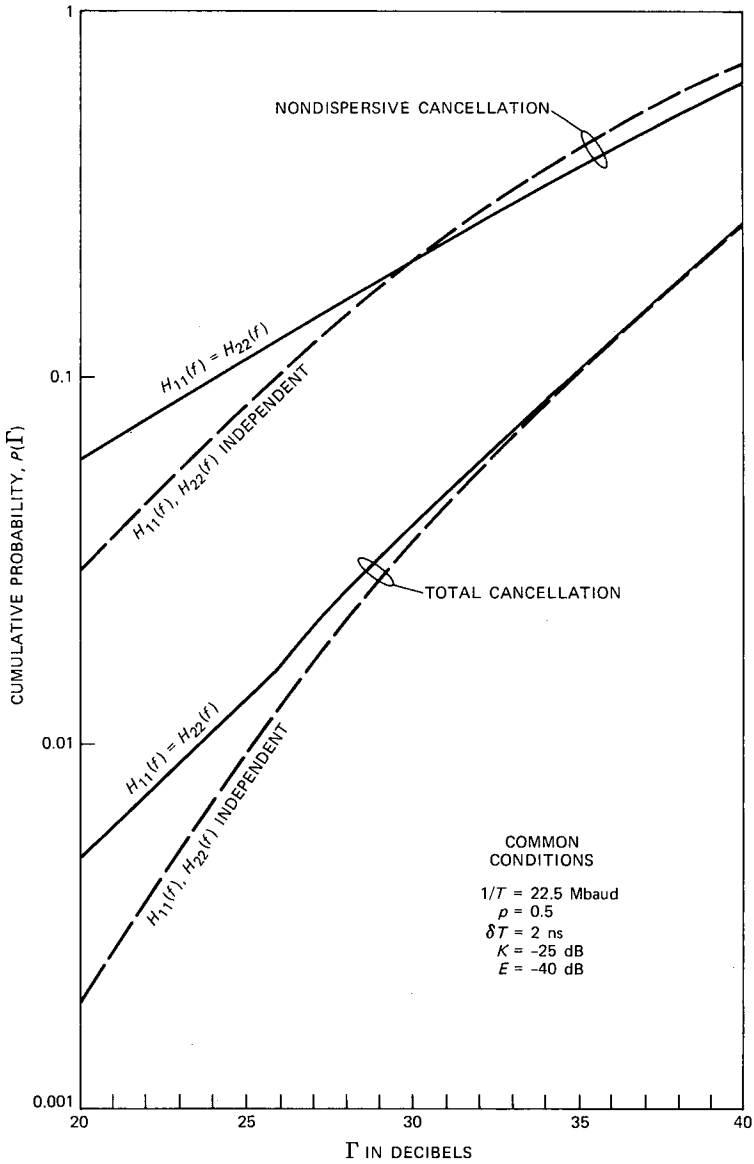

Fig. 5—Cumulative probability functions for Γ. Same conditions as in Fig. 4, except that p and δT are fixed at 0.5 and 2 ns, and results are shown for both totally dependent and totally independent co-pol response functions.

$H_{12}H_{21}$. If H_{11} and H_{22} are independent, however, there is a chance that H_{22} will be strong enough at such times to avoid this near-cancellation. The statistical effect of all this is reflected in the comparative results of Fig. 5.

4.4 *Influence of channel coupling parameters K and E*

Figure 6 shows results for both nondispersive and total cancellation as K and E range over the sets of values we have specified for them. Note that these particular results are for $1/T = 22.5$ Mbaud and $H_{11}(f) = H_{22}(f)$.

For nondispersive cancellation, each heavy line contains results for a particular E and all K below -25 dB. The negligible influence of K over this range is apparent. However, E is another matter. As this quantity decreases in 5-dB steps from -35 dB, the probability curves shift to the right by nearly 5 dB. These features reflect the fact that nondispersive cancellation virtually eliminates the effect of the cross-coupling gain component $kH_{11}(f)$ in (6) [remember that $H_{22}(f) = H_{11}(f)$ in these calculations] but is less effective against the second component, whose mean-square value in decibels is E. This reveals yet another way in which precision in the channel model is needed to estimate nondispersive canceller performance.

For the case of total cancellation, on the other hand, the lower band in Fig. 6 shows how much that need is attenuated. Even so, this band widens measurably as E decreases below -45 dB. The point is made clear by the dotted curve, for $K = E = -\infty$, which is equivalent to the case of single-pol transmission (i.e., no input CPI) and ideal MMSE equalization.

We now see how closely dual-pol outage performance comes to that for single-pol operation when total cross-pol cancellation is used. We can also make a limited comparison between the cascaded approach (i.e., canceller and equalizer in tandem) and the optimum linear receiver (i.e., jointly optimizing $\{G_{11}(f), G_{12}(f), G_{21}(f), G_{22}(f)\}$ against both CPI and multipath dispersion, thereby eliminating the separate equalizer). The latter case is treated comprehensively by Amitay and Salz in Ref. 1. In that paper, the probability functions are plotted against *spectral efficiency*, in b/s/Hz, and so the following correspondences apply: the abscissa values of 4 and 6 b/s/Hz in Ref. 1 correspond closely to $\Gamma = 20$ and 26 dB, respectively, in the present paper. Now assuming that $E = -35$ dB and $1/T = 30$ Mbaud, Fig. 3 of Ref. 1 shows the outage probability for the optimal linear receiver to be roughly four times higher than for single-pol transmission when the spectral efficiency is 4 b/s/Hz, and roughly two times higher when the spectral efficiency is 6 b/s/Hz. The corresponding results in the present study for $\Gamma = 20$ and 26 dB are quite similar and, for higher abscissa values, the similarities are even greater. While recognizing that the two studies used somewhat different models and methods of analysis, and entirely different random numbers in their Monte Carlo

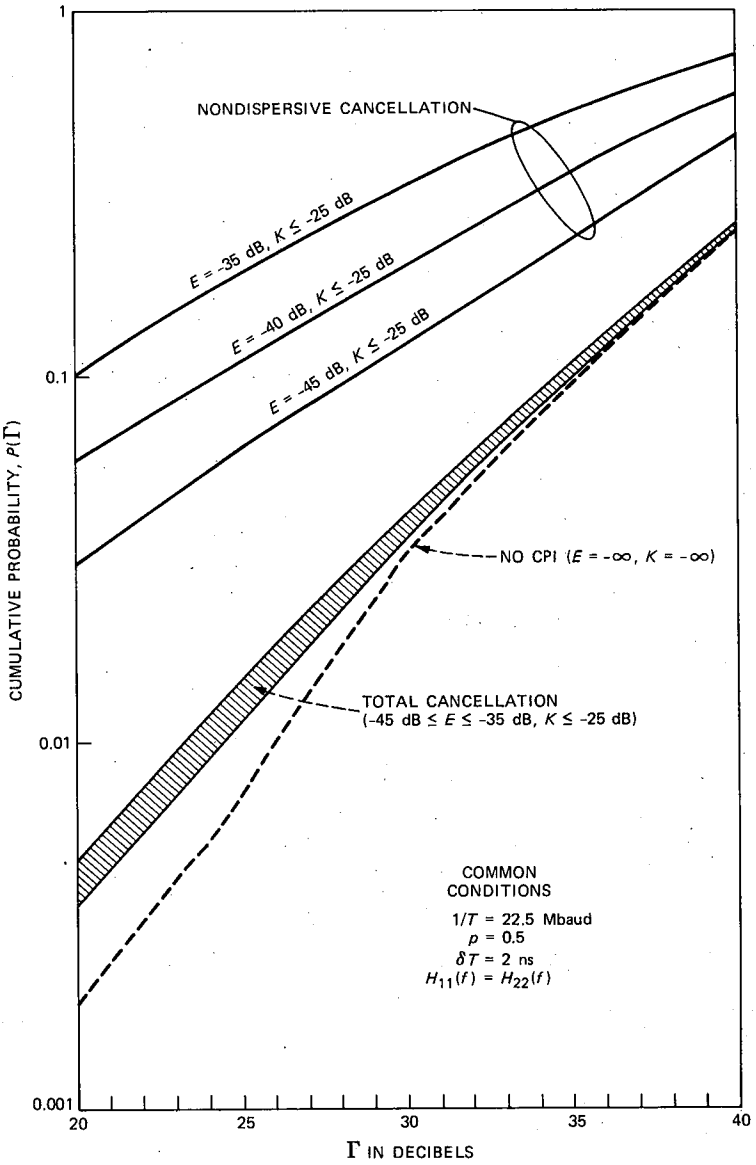

Fig. 6—Cumulative probability functions for Γ. Same conditions as in Fig. 4, except that p and δT are fixed at 0.5 and 2 ns, and K and E are parameters. Note the dotted curve "No CPI," which corresponds to an ideally equalized single-pol channel.

simulations, we perceive a general truth in this comparison: specifically, the cascaded approach, in which cancellation and equalization are functionally separate, leads to outage statistics very close to those for optimal linear reception.

4.5 Influence of system design parameters α and CNR

All of the results in Figs. 3 through 6 are for $\alpha = 0$ and CNR $= 2 \times 10^6$ (63 dB). Nevertheless, we can say something about the influences of these parameters. From previous studies,[11] for example, we know that α has a very small effect on outage probability over the practical range $0 < \alpha \leq 0.5$. Also, the curves for total cancellation would essentially shift X dB to the right (or left) for every X-dB increase (or decrease) in CNR. This is because the residual distortion in the case of total cancellation followed by MMSE equalization is almost entirely thermal noise. In the case of nondispersive cancellation, wherein the dominant residual distortion is uncancelled CPI, this sensitivity of the results to CNR would be sharply reduced.

V. SUMMARY AND CONCLUSION

We have used analysis and Monte Carlo simulation to estimate conditional outage probabilities in dual-pol digital radio as functions of a detection measure (Γ) that can be related to the number of modulation levels and the bit error rate. In performing the simulations, we have resorted to a statistical model for the dual-pol channel that lacks a firm empirical basis. This results unavoidably from the current incomplete status of dual-pol channel measurement and modeling. We have dealt with this limitation, in part, by treating various uncertain aspects of the model parametrically.

The main findings of this study can be summarized as follows:

- Obtaining reliable estimates of outage probability for the case of nondispersive cancellation requires accurate, detailed descriptions of the underlying channel model. The outage performance of this cancellation approach is also quite sensitive to bandwidth (or symbol rate).
- In the case of total cancellation, by contrast, outage performance is insensitive to many details of the channel model as well as to symbol rate.
- While far superior to no cancellation, nondispersive cancellation leads to outage probabilities an order-of-magnitude greater than does total cancellation. Nonetheless, it may find applications where symbol rates are low (less than 5 Mbaud) and the outage requirements are liberal.
- The outage statistics for total cancellation followed by ideal equalization are fairly close to those for single-pol transmission, wherein there is no cross-pol interference to cancel.
- More significantly, total cancellation in cascade with ideal equalization appears to produce outage statistics very close to those for optimal linear reception, wherein the effects of cross-pol interfer-

ence and multipath dispersion are jointly minimized in the same receiver stage. Use of the cascade approach, therefore, may permit such benefits as design simplicity, manufacturing economy, and operational flexibility with no serious loss in performance.

VI. ACKNOWLEDGMENT

I am grateful to Lisa J. (Domenico) Case for her help in executing the computer simulation/analysis programs.

REFERENCES

1. N. Amitay and J. Salz, "Linear Equalization Theory in Digital Data Transmission Over Dually Polarized Fading Radio Channels," AT&T Bell Lab. Tech. J., *63,* No. 10, Part 1 (December 1984), pp. 2215–59.
2. W. D. Rummler, "A New Selective Fading Model: Application to Propagation Data," B.S.T.J., *58,* No. 7 (May–June 1979), pp. 1037–71.
3. W. D. Rummler, "More on the Multipath Fading Channel Model," IEEE Trans. Commun., *COM-29,* No. 3 (March 1981), pp. 346–52.
4. L. J. Greenstein and B. A. Czekaj, "A Polynomial Model for Multipath Fading Channel Responses," B.S.T.J., *59,* No. 7 (September 1980), pp. 1197–225.
5. J. C. Campbell and R. P. Coutts, "Outage Prediction of Digital Radio Systems," Electron. Lett., *18,* No. 25/26 (December 1982), pp. 1071–2.
6. K. T. Wu, "Measured Statistics of Multipath Dispersion of Cross Polarization Interference," Paper 46.3, Int. Conf. Commun., May 14–17, 1984, Amsterdam.
7. N. Amitay and L. J. Greenstein, "Multipath Outage Performance of Digital Radio Receivers Using Finite-Tap Adaptive Equalizers," IEEE Trans. Commun., *COM-32,* No. 5 (May 1984), pp. 597–608.
8. S. H. Lin, "Impact of Microwave Depolarization During Multipath Fading on Digital Radio Performance," B.S.T.J., *56,* No. 5 (May 1977), pp. 645–74.
9. M. L. Steinberger, "Design of a Terrestrial Cross Pol Canceller," Paper 2B.6, Int. Conf. Commun., June 13–17, 1982, Philadelphia, Pa.
10. M. Liniger, "Sweep Measurements of Multipath Effects on Cross-Polarized RF-Channels Including Space Diversity," Paper 45.7, GLOBECOM '84, November 26–29, 1984, Atlanta, Ga.
11. W. C. Wong and L. J. Greenstein, "Multipath Fading Models and Adoptive Equalizers in Microwave Digital Radio," IEEE Trans. Commun., *COM-32,* No. 8 (August 1984), pp. 928–34.
12. R. W. Lucky, J. Salz, and E. J. Weldon, Jr., *Principles of Data Communication,* New York: McGraw-Hill, 1968.
13. G. J. Foschini and J. Salz, "Digital Communications Over Fading Radio Channels," B.S.T.J., *62,* No. 2, Part 1 (February 1983), pp. 429–56.

AUTHOR

Larry J. Greenstein, B.S.E.E., 1958, M.S.E.E., 1961, and Ph.D. (Electrical Engineering), 1967, Illinois Institute of Technology; AT&T Bell Laboratories, 1970—. Mr. Greenstein currently heads the Radio Systems Research Department at Crawford Hill in Holmdel, N.J. His most recent work has dealt with communications satellites, mobile telephony, microwave digital radio and optical communications. His previous work was on digital encoding, digital filtering, and, at IIT Research Institute before 1970, airborne radar. Member, Eta Kappa Nu, Tau Beta Pi, and Sigma Xi; Senior Member, IEEE; Senior Technical Editor, IEEE Communications Magazine; co-recipient, IEEE Communications Society's 1984 Prize Paper Award in Communications Systems.